

# Modelling Baryon Acoustic Oscillations with Perturbation Theory and Stochastic Halo Biasing

Francisco-Shu Kitaura<sup>1\*</sup>, Gustavo Yepes<sup>2</sup> & Francisco Prada<sup>3,4,5</sup>

<sup>1</sup>*Leibniz-Institut für Astrophysik Potsdam (AIP), An der Sternwarte 16, D-14482 Potsdam, Germany*

<sup>2</sup>*Departamento de Física Teórica, Universidad Autónoma de Madrid, Cantoblanco, 28049, Madrid, Spain*

<sup>3</sup>*Campus of International Excellence UAM+CSIC, Cantoblanco, E-28049 Madrid, Spain*

<sup>4</sup>*Instituto de Física Teórica, (UAM/CSIC), Universidad Autónoma de Madrid, Cantoblanco, E-28049 Madrid, Spain*

<sup>5</sup>*Instituto de Astrofísica de Andalucía (CSIC), Glorieta de la Astronomía, E-18080 Granada, Spain*

26 September 2018

## ABSTRACT

In this work we investigate the generation of mock halo catalogues based on perturbation theory and nonlinear stochastic biasing with the novel PATCHY-code. In particular, we use Augmented Lagrangian Perturbation Theory (ALPT) to generate a dark matter density field on a mesh starting from Gaussian fluctuations and to compute the peculiar velocity field. ALPT is based on a combination of second order LPT (2LPT) on large scales and the spherical collapse model on smaller scales. We account for the systematic deviation of perturbative approaches from  $N$ -body simulations together with halo biasing adopting an exponential bias model. We then account for stochastic biasing by defining three regimes: a low, an intermediate and a high density regime, using a Poisson distribution in the intermediate regime and the negative binomial distribution –including an additional parameter– to model over-dispersion in the high density regime. Since we focus in this study on massive halos, we suppress the generation of halos in the low density regime. The various nonlinear and stochastic biasing parameters, and density thresholds are calibrated with the large BigMultiDark  $N$ -body simulation to match the power spectrum of the corresponding halo population. Our model effectively includes only five parameters, as they are additionally constrained by the halo number density. Our mock catalogues show power spectra, both in real- and redshift-space, which are compatible with  $N$ -body simulations within about 2% up to  $k \sim 1 h \text{ Mpc}^{-1}$  at  $z = 0.577$  for a sample of halos with the typical BOSS CMASS galaxy number density. The corresponding correlation functions are compatible down to a few Mpc. We also find that neglecting over-dispersion in high density regions produces power spectra with deviations of 10% at  $k \sim 0.4 h \text{ Mpc}^{-1}$ . These results indicate the need to account for an accurate statistical description of the galaxy clustering for precise studies of large-scale surveys.

**Key words:** (cosmology:) large-scale structure of Universe – galaxies: clusters: general – catalogues – galaxies: statistics

## 1 INTRODUCTION

The new generation of galaxy surveys request precise numerical simulations of structure formation to compare theoretical models to observations. This is computationally very demanding as the parameter space one needs to cover is extremely large, ranging from varying the cosmological parameters, over modelling different biased tracers, to account for cosmic variance (for large-volume  $N$ -body simulations see e.g. Kim et al. 2009; Prada et al. 2012; Angulo et al. 2012; Alimi et al. 2012; Watson et al. 2013). As an al-

ternative to run  $N$ -body cosmological simulations for each parameter set, one can calibrate approximate structure formation models to  $N$ -body solutions and scan the parameter space using the more efficient schemes. A number of approaches has been proposed in the literature for the generation of mock galaxy catalogues based on Lagrangian Perturbation Theory (LPT), such as PINOCCHIO (Monaco et al. 2002, 2013) or PTHALOS (Scoccimarro & Sheth 2002; Manera et al. 2013). It has been shown that perturbation theory can provide an accurate approach to model Baryon Acoustic Oscillations (BAOs) (Tassev & Zaldarriaga 2012). The uncertainty of a few Mpc in the position of dark matter particles (or halos) following the approximate schemes is translated into a damping

\* E-mail: kitaura@aip.de, Karl-Schwarzschild-fellow

of the power spectrum, which may be modeled by a Gaussian smoothing of the typical uncertainty scale (Monaco et al. 2013). As a consequence, the power spectra predicted by perturbation theory lie below the linear power spectrum instead of developing the characteristic nonlinear excess of power with respect to the linear power spectrum at modes  $k \gtrsim 0.1 h \text{ Mpc}^{-1}$ . Interesting alternatives have been recently proposed, such as re-scaling  $N$ -body simulations to account for a change in the cosmological parameters (Angulo & White 2010), compute covariance matrices from a set of small-volume simulations (Schneider et al. 2011), or including 2LPT within the Vlasov equations solver to speed up  $N$ -body codes (COLA, Tassev et al. 2013). In this letter, we propose to use an extremely efficient approach based on low resolution one-step perturbation theory solvers. We rely on Augmented LPT (ALPT), which is based on a combination of second order LPT on large scales with the spherical collapse model on smaller scales, suppressing in this way shell-crossing with an improved modelling of filaments (Kitaura & Heß 2013). In this work, we introduce the peculiar velocity within this formalism to model redshift-space distortions.

To account for the missing power of perturbative approaches at high modes, and at the same time for the scale-dependent bias of halos, we use an exponential bias (Cen & Ostriker 1993). Such a model has been recently proposed to sample halos below the resolution of dark matter simulations (de la Torre & Peacock 2013). This model is related to the lognormal model (Coles & Jones 1991), and thus to the linear component of the density field (Kitaura & Angulo 2012), solving the negative densities problem (Kitaura et al. 2010) of Fry & Gaztanaga (1993)'s formulation. Here, we propose to model the statistics of halos with a Poissonian and a negative binomial distribution function depending on the density regime. The required parameters in our model are calibrated with one of the new set of the publicly available BigMultiDark simulations<sup>1</sup> (Heß et al in prep).

Our approach is not only useful to generate mock catalogues, but also for inference analysis of the large-scale structure (density fields, power spectra, etc), improving previous models based on a linear bias and on the Poisson assumption (see e.g. Kitaura & Enßlin 2008; Kitaura et al. 2010).

This letter is structured as follows: in the next section (§2) we present our method. We then show (§3) our numerical experiments calibrating our mock catalogues with  $N$ -body simulations. Finally (§4) we present our conclusions and discussion.

## 2 METHOD

Our approach combines an efficient structure formation model with a local, nonlinear, scale-dependent and stochastic biasing scheme. The resulting computer code is dubbed PATCHY (Perturbation Theory Catalog generator of Halo and galaxy distributions).

### 2.1 Structure formation model

We use Augmented Lagrangian Perturbation Theory (ALPT) to simulate structure formation (Kitaura & Heß 2013). In this approximation the displacement field  $\Psi(\mathbf{q}, z)$ , mapping a distribution of dark matter particles at initial Lagrangian positions  $\mathbf{q}$  to the final Eulerian positions  $\mathbf{x}(z)$  at redshift  $z$  ( $\mathbf{x}(z) = \mathbf{q} + \Psi(\mathbf{q}, z)$ ), is split

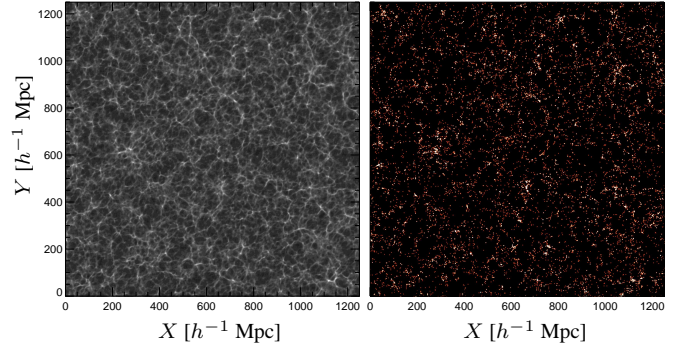


**Figure 1.** Slices of thickness  $20 h^{-1} \text{ Mpc}$  and  $1250 h^{-1} \text{ Mpc}$  side of a PATCHY simulation through the dark matter density field (on the left) and through the corresponding halo field (on the right). The logarithm of the density fields are shown. Lighter regions represent higher densities.

into a long-range  $\Psi_L(\mathbf{q}, z)$  and a short-range component  $\Psi_S(\mathbf{q}, z)$ , i.e.  $\Psi(\mathbf{q}, z) = \Psi_L(\mathbf{q}, z) + \Psi_S(\mathbf{q}, z)$ . We rely on 2LPT for the long-range component:

$$\Psi_{2\text{LPT}} = -D\nabla\phi^{(1)} + D_2\nabla\phi^{(2)}, \quad (1)$$

where  $D$  is the linear growth factor and  $D_2 \simeq -3/7 \Omega^{-1/143} D^2$  (for details on 2LPT see Buchert 1994; Bouchet et al. 1995; Catelan 1995). The potentials  $\phi^{(1)}$  and  $\phi^{(2)}$  are obtained by solving a pair of Poisson equations:  $\nabla^2\phi^{(1)} = \delta^{(1)}$ , where  $\delta^{(1)}$  is the linear overdensity, and  $\nabla^2\phi^{(2)} = \delta^{(2)}$ . The second order nonlinear term  $\delta^{(2)}$  is fully determined by the linear overdensity field  $\delta^{(1)}$  through the following quadratic expression:

$$\delta^{(2)} \equiv \sum_{i>j} \left( \phi_{,ii}^{(1)} \phi_{,jj}^{(1)} - [\phi_{,ij}^{(1)}]^2 \right), \quad (2)$$

where we use the following notation  $\phi_{,ij} \equiv \partial^2\phi/\partial q_i\partial q_j$ , and the indices  $i, j$  run over the three Cartesian coordinates.

The resulting displacement field is filtered with a kernel  $\mathcal{K}$ :  $\Psi_L(\mathbf{q}, z) = \mathcal{K}(\mathbf{q}, r_S) \circ \Psi_{2\text{LPT}}(\mathbf{q}, z)$ . We apply a Gaussian filter  $\mathcal{K}(\mathbf{q}, r_S) = \exp(-|\mathbf{q}|^2/(2r_S^2))$ , with  $r_S$  being the smoothing radius. We use the spherical collapse approximation to model the short-range component  $\Psi_S(\mathbf{q}, z)$  (see Bernardeau 1994; Mohayaee et al. 2006; Neyrinck 2013):  $\Psi_S(\mathbf{q}, z) = (1 - \mathcal{K}(\mathbf{q}, r_S)) \circ \Psi_{\text{SC}}(\mathbf{q}, z)$ , where

$$\Psi_{\text{SC}} = \nabla\nabla^{-2} \left[ 3 \left( \left( 1 - \frac{2}{3} D\delta^{(1)} \right)^{1/2} - 1 \right) \right]. \quad (3)$$

The combined ALPT displacement field

$$\Psi_{\text{ALPT}}(\mathbf{q}, z) = \mathcal{K}(\mathbf{q}, r_S) \circ \Psi_{2\text{LPT}}(\mathbf{q}, z) + (1 - \mathcal{K}(\mathbf{q}, r_S)) \circ \Psi_{\text{SC}}(\mathbf{q}, z) \quad (4)$$

is used to move a set of homogeneously distributed particles from Lagrangian initial conditions to the Eulerian final ones. We then grid the particles following a clouds-in-cell scheme to produce a smooth density field  $\delta^{\text{ALPT}}$ .

### 2.2 Deterministic biasing

The relation between the halo distribution and the underlying dark matter density field is known to be nonlinear, nonlocal and stochastic (Press & Schechter 1974; Peacock & Heavens 1985; Bardeen et al. 1986; Fry & Gaztanaga 1993; Mo & White 1996; Dekel & Lahav 1999; Sheth & Lemson 1999; Seljak 2000; Berlind & Weinberg 2002; Smith et al. 2007; Desjacques et al.

<sup>1</sup> <http://www.multidark.org>

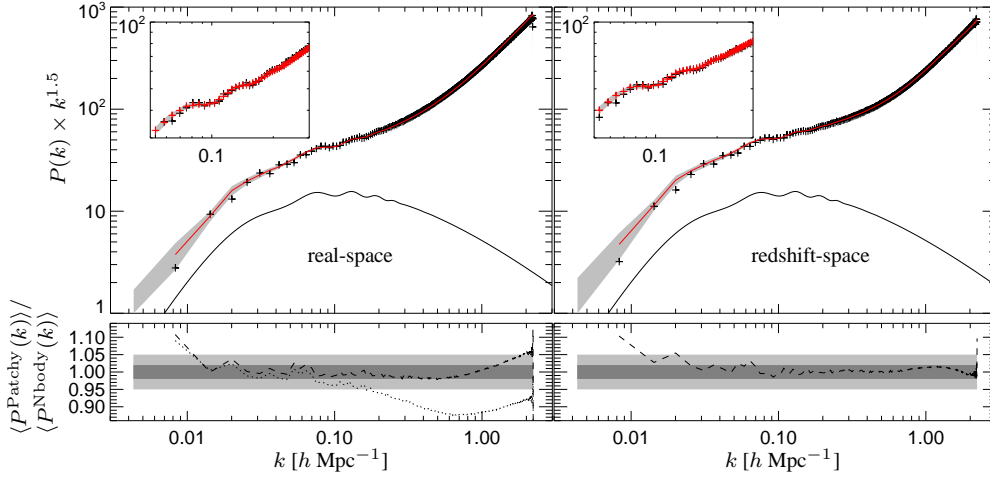


**Figure 2.** Power spectra obtained with PATCHY vs. BigMultiDark at  $z = 0.577$  for a halo sample with number density  $3.6 \times 10^{-4} \text{ Mpc}^{-3} h^3$  in real-space (on the left) and in redshift-space (on the right). The red line corresponds to the mean of 50 PATCHY realizations with the corresponding 1-sigma region in grey. The linear power spectrum is also shown (solid black line) as well as the mean over 8 sub-volumes of the BigMultiDark simulation. Bottom: Ratio between the mean of the PATCHY realizations and the mean of the  $N$ -body sub-volumes. Dotted curve: only Poisson, dashed curves: includes negative-binomial PDF. Regions within 2% are indicated by the dark grey area and 5% by the lighter one.

2010; Beltrán Jiménez & Durrer 2011; Valageas & Nishimichi 2011; Elia et al. 2012; Chan et al. 2012; Baldauf et al. 2012, 2013). We will neglect for the time being nonlocal biasing. To account for nonlinear biasing we consider an exponential expression which includes only 2 parameters (with only one free parameter),  $f_N$  and  $\alpha$ , to get the expected number counts of halos in a cell  $i$  from the density field (Cen & Ostriker 1993; de la Torre & Peacock 2013), i.e.

$$\lambda_i \equiv \langle N_i \rangle = f_N \times (1 + \delta_i^{\text{ALPT}})^\alpha, \quad (5)$$

where the brackets stand for the ensemble average over the realization of halos given a particular probability distribution function (PDF)  $P(N_i | \lambda_i, \{p_i\})$  with a set of parameters  $\{p_i\}$ :  $\langle N_i \rangle = \sum_{N_i=0}^{\infty} P(N_i | \lambda_i, \{p_i\}) N_i$  (see next subsection). The parameter  $\alpha$  controls the nonlinear, scale-dependent bias, while  $f_N$  controls the halo number density. We note that for the unbiased case ( $\alpha = 1$ )  $f_N$  is equal to the number density  $\bar{N} \equiv \langle \lambda \rangle_V = \langle f_N \times (1 + \delta^{\text{ALPT}}) \rangle_V = f_N$ , where  $\langle \dots \rangle_V$  is the ensemble average over a sufficiently large volume  $V$ , so that  $\langle \delta^{\text{ALPT}} \rangle_V = 0$ . Accordingly, we find  $f_N$  being in general given by:

$$f_N = \bar{N} / \langle (1 + \delta_i^{\text{ALPT}})^\alpha \rangle_V. \quad (6)$$

### 2.3 Stochastic biasing

The halo distribution is a discrete sample of the continuous underlying dark matter distribution. To account for the shot noise one could do Poissonian realizations of the halo density field as given by the deterministic bias and the dark matter field (see e.g. de la Torre & Peacock 2013). However, it is known that the excess probability of finding halos in high density regions generates over-dispersion (Somerville et al. 2001; Casas-Miranda et al. 2002), underdense regions are under-dispersed and there is an intermediate regime (mainly filaments) in which Poissonity approximately holds. Therefore we define three regimes: a low density ( $\delta^{\text{ALPT}} > \delta^{\text{low}}$ ), an intermediate ( $\delta^{\text{low}} < \delta^{\text{ALPT}} < \delta^{\text{high}}$ ) and a high density regime ( $\delta^{\text{ALPT}} > \delta^{\text{high}}$ ). We use a Poisson distribu-

tion in the intermediate regime:

$$P(N_i | \lambda_i) = \frac{\lambda_i^{N_i}}{N_i!} \exp(-\lambda_i), \quad (7)$$

and the negative binomial (NB) PDF (for non-Poissonian distributions see Saslaw & Hamilton 1984; Sheth 1995) including an additional parameter  $\beta$  to model over-dispersion in the high density regime:

$$P(N_i | \lambda_i, \beta) = \frac{\lambda_i^{N_i}}{N_i!} \frac{\Gamma(\beta + N_i)}{\Gamma(\beta) \Gamma(\beta + \lambda)^{N_i}} \frac{1}{(1 + \lambda/\beta)^\beta}. \quad (8)$$

This PDF tends towards the Poisson distribution for  $\beta \rightarrow \infty$ . The NB is also very close to the Poissonian distribution for low  $\lambda$  values. For this reason we could consider only one threshold density  $\delta^{\text{th}} = \delta^{\text{low}} = \delta^{\text{high}}$ , reducing the number of parameters in our model. We will investigate this further in future works. Since we focus in this study on massive halos to model Luminous Red Galaxies (LRGs), we then suppress the generation of halos in the low density regime. A Bayesian inference algorithm based on a combination of these PDFs will appear in a forthcoming publication.

### 2.4 Redshift-space distortions

The mapping between Eulerian real-space  $\mathbf{x}(z)$  and redshift-space  $\mathbf{s}(z)$  is given by:  $\mathbf{s}(z) = \mathbf{x}(z) + \mathbf{v}_r(z)$ , with  $\mathbf{v}_r \equiv (\mathbf{v} \cdot \hat{\mathbf{r}}) \hat{\mathbf{r}} / (Ha)$ ; where  $\hat{\mathbf{r}}$  is the unit sight line vector,  $H$  the Hubble constant,  $a$  the scale factor, and  $\mathbf{v} = \mathbf{v}(\mathbf{x})$  the 3-d velocity field interpolated at the position of each halo in Eulerian-space  $\mathbf{x}$  using the displacement field  $\Psi_{\text{ALPT}}(\mathbf{q}, z)$ . We split the peculiar velocity field into a coherent  $\mathbf{v}^{\text{coh}}$  and a (quasi-) virialized component  $\mathbf{v}_\sigma$ :  $\mathbf{v} = \mathbf{v}^{\text{coh}} + \mathbf{v}_\sigma$ . The coherent peculiar velocity field is computed in Lagrangian-space from the linear Gaussian field  $\delta^{(1)}(\mathbf{q})$  using the ALPT formulation consistently with the displacement field (see Eq. 4):

$$\mathbf{v}_{\text{ALPT}}^{\text{coh}}(\mathbf{q}, z) = \mathcal{K}(\mathbf{q}, r_S) \circ \mathbf{v}_{2\text{LPT}}(\mathbf{q}, z) + (1 - \mathcal{K}(\mathbf{q}, r_S)) \circ \mathbf{v}_{\text{SC}}(\mathbf{q}, z) \quad (9)$$

For the second order LPT component  $\mathbf{v}_{2\text{LPT}}$  we refer to e. g. Buchert & Ehlers (1993); Bouchet et al. (1995):

$$\mathbf{v}_{2\text{LPT}} = -fHaD\nabla\phi^{(1)} + f_2HaD_2\nabla\phi^{(2)}, \quad (10)$$

where  $f_i = d \ln D_i / d \ln a$  ( $D \equiv D_1$ ,  $f \equiv f_1 \approx \Omega^{5/9}$ ,  $f_2 \approx 2\Omega^{6/11}$ ).

The spherical collapse component is obtained by performing the time derivative of Eq. 3:

$$v_{\text{SC}} = \nabla \nabla^{-2} \left[ -f H a D \delta^{(1)} \left( 1 - \frac{2}{3} D \delta^{(1)} \right)^{-1/2} \right]. \quad (11)$$

We use the high correlation between the local density field and the velocity dispersion to model the displacement due to (quasi-) virialized motions. Effectively, we sample a Gaussian distribution function ( $\mathcal{G}$ ) with a dispersion given by  $\sigma_v \propto (1 + b^{\text{ALPT}} \delta^{\text{ALPT}}(\mathbf{x}))^\gamma$ . Consequently,

$$v_r^\sigma \equiv (v^\sigma \cdot \hat{r}) \hat{r} / (H a) = \mathcal{G} \left( g \times \left( 1 + b^{\text{ALPT}} \delta^{\text{ALPT}}(\mathbf{x}) \right)^\gamma \right) \hat{r}, \quad (12)$$

(see Kitaura 2007; Kitaura & Enßlin 2008; Heß et al. 2013). The linear bias between the ALPT approximation and the full  $N$ -body solution is given by  $b^{\text{ALPT}}$  and is close to unity for scales of a few Mpc (see Heß et al. 2013). The parameters  $g$  and  $\gamma$  have been adjusted to fit the damping effect in the power-spectrum in redshift-space as found in the BigMultiDark  $N$ -body simulation. In closely virialized systems the kinetic energy approximately equals the gravitational energy and a Keplerian law predicts  $\gamma$  close to 0.5 (see Kitaura 2007; Heß & Kitaura in prep), leaving only the proportionality constant  $g$  as a free parameter in our model.

### 3 NUMERICAL EXPERIMENTS

We use a reference halo catalogue at redshift  $z = 0.577$  extracted from one of the BigMultiDark simulations (Heß et al in prep), which was performed using GADGET-2 (Springel 2005) with  $3840^3$  particles on a volume of  $(2500 h^{-1} \text{ Mpc})^3$  assuming  $\Lambda$ CDM-cosmology with  $\{\Omega_{\text{M}} = 0.29, \Omega_{\text{K}} = 0, \Omega_{\Lambda} = 0.71, \Omega_{\text{B}} = 0.047, \sigma_8 = 0.82, w = -1, n_s = 0.95\}$  and a Hubble constant ( $H_0 = 100 h \text{ km s}^{-1} \text{ Mpc}^{-1}$ ) given by  $h = 0.7$ . Halos were produced based on density peaks including substructures using the Bound Density Maximum (BDM) halo finder (Klypin & Holtzman 1997) and then selected according to a maximum circular velocity larger than  $350 \text{ km s}^{-1}$  to match the number density of BOSS CMASS galaxies (Nuza et al. 2013). For the impact of these selection criteria in the clustering and scale-dependent bias see Prada et al (in prep).

We make a partition of the BigMultiDark box into 8 sub-volumes of equal size  $(1250 h^{-1} \text{ Mpc})^3$ . This permits us to get rough estimates of the variance in the power spectra and correlation functions due to cosmic variance. Since our approach yields number counts in cells on a mesh, we define the reference power spectrum as the mean of the ones corresponding to the halo overdensity field in the sub-volumes gridded with nearest-grid-point (NGP). We choose a mesh of  $512^3$  cells to reach a resolution of cell size  $2.4 h^{-1} \text{ Mpc}$ . We have explored the parameter space of our model  $\{\alpha, \beta, \delta^{\text{low}}, \delta^{\text{high}}, g\}$  running PATCHY with  $512^3$  particles in volumes of  $(1250 h^{-1} \text{ Mpc})^3$  to maximize the fit to the reference power spectrum in the relevant range for BAOs. This leads to an inconsistency with the large-scale modes which are included in BigMultiDark, but not in the PATCHY realizations. We will investigate the impact of this approximation in a future work. Our criterion for the parameter selection is based on reaching better than 2% accuracy in the range  $0.07 < k < 0.4 h \text{ Mpc}^{-1}$ . Using a set of parameters, which meet our criteria, we perform 50 random seeded realizations with PATCHY. We have checked that the halo number

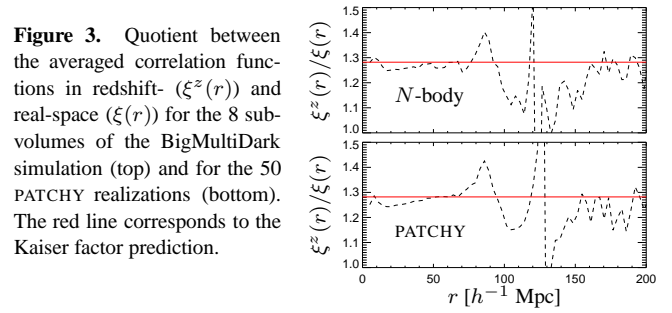


**Figure 3.** Quotient between the averaged correlation functions in redshift- ( $\xi^z(r)$ ) and real-space ( $\xi(r)$ ) for the 8 sub-volumes of the BigMultiDark simulation (top) and for the 50 PATCHY realizations (bottom). The red line corresponds to the Kaiser factor prediction.

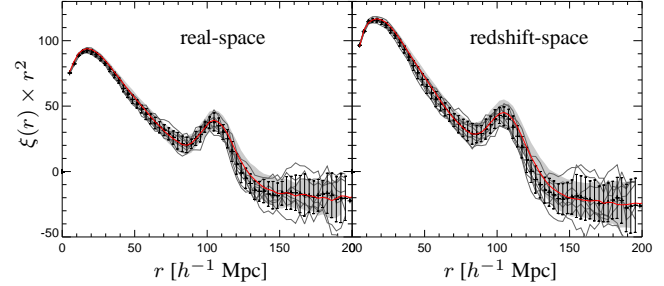


**Figure 4.** Correlation functions of the PATCHY simulations vs the BigMultiDark  $N$ -body simulation. The red line corresponds to the mean of the PATCHY realizations with the corresponding 1-sigma region in grey. Crosses: mean over the BigMultiDark sub-volumes. The error bars indicate 1-sigma means for the  $N$ -body case. Each of the 8 sub-volumes drawn from the  $N$ -body simulation is represented by the grey lines. The left panel shows real-space, while the right panel shows redshift-space.

density from the realizations is compatible with the expected number density (about 70% of the realizations lie within the 1-sigma region of the  $N$ -body simulation with a very close mean). A slice through the distribution of the dark matter and the corresponding halo sample are presented in Fig. 1. The dark matter slice clearly shows the nonlinear cosmic web. Looking carefully, one can distinguish resolution effects in voids. However, these should not affect our mocks as we do not consider massive halos in low density regions. This issue should be revisited when generating catalogues for low mass halos. Fig. 2 shows the power spectra comparing the results between PATCHY and the BigMultiDark  $N$ -body simulation. On the left panel we find an agreement between the model and the reference power spectrum within 2% up to  $k \sim 1 h \text{ Mpc}^{-1}$  in real-space. The same is shown in redshift-space on the right panel. We have checked the PATCHY performance neglecting over-dispersion using the Poisson distribution also in the high density regime. In this case the deviation from the reference power spectrum can be larger than 10%, being in particular above 10% at  $k = 0.4 h \text{ Mpc}^{-1}$  (see dotted line in the left-lower panel on Fig. 2). Fig. 3 shows that the Kaiser factor  $K$  (Kaiser 1987)<sup>2</sup>, the BAO damping, and the excess of power at scales lower than the BAO peak, are well reproduced with our redshift-space distortion model. The correlation functions for both real- and redshift-space are shown in Fig. 4. We can see that in all bins PATCHY is compatible, within the error bars, with the BigMultiDark  $N$ -body simulation down to scales  $\lesssim 5 h^{-1} \text{ Mpc}$ . The dispersion in the correlation functions from the  $N$ -body and the PATCHY realizations are remarkably similar.

<sup>2</sup>  $K = 1 + \frac{2}{3}\beta + \frac{1}{5}\beta^2 \sim 1.28$ , with  $\beta = f/b$ ,  $f$  being the growth rate, and  $b \sim 2$  being the linear bias for our mock LRG sample.

## 4 CONCLUSIONS AND DISCUSSION

In this work we have combined structure formation perturbation theory with a local, nonlinear, stochastic bias including redshift-space distortions to generate mock halo catalogues of a given number density using the novel PATCHY-code. We have also shown the importance of treating over-dispersion in high density regions to reach precisions of about 2% in the power spectrum. The advantage of our approach is manifold. First, we use an improved efficient one-step solver (Augmented Lagrangian Perturbation Theory: ALPT) yielding a smooth density field on a mesh. Second, we use a statistical model applied to that field to produce a distribution of halos with power spectra matching those obtained from the BigMultiDark  $N$ -body simulations, as opposed to other methods, which rely on the halos obtained with the corresponding approximation (e.g. PTHALOS, PINOCCHIO or COLA). In this way, we circumvent two problems: the inaccuracy of the perturbative approach and the large number of particles required to resolve the halo population of interest within volumes. In our tests we have used  $\sim 50$  times less particles than for the BigMultiDark simulation in the corresponding volume. Finally, we have modeled redshift-space distortions, reproducing the correlation function of  $N$ -body simulations with the same level of accuracy as in real-space.

Still a number of issues have to be investigated, such as the performance of the method as a function of redshift (including light-cones), cosmological parameters, nonlocal bias, and different halo number densities. Higher order statistics (skewness, kurtosis, three-point correlation functions or bispectrum) are expected to be reasonably well modeled as we are using improved versions of 2LPT correcting for the damped power spectrum. We will investigate all these issues in detail for mass production of mock catalogues and plan to make PATCHY publicly available.

In summary, PATCHY proves to be an especially efficient and accurate method based on perturbation theory to generate mock catalogues including nonlinear, scale-dependent and stochastic biasing with redshift-space distortions, which can be used to compute covariance matrices for large galaxy surveys.

## Acknowledgments

FSK thanks V. Müller for encouraging discussions. Special thanks to A. Klypin, S. Heß, S. Gottlöber and C. Scoccola. We thank R. E. Angulo and C. H. Chuang for comments on the manuscript. The work was initiated under the HPC-Europa2 project (project number: 228398) with the support of the European Commission - Capacities Area - Research Infrastructures. The MultiDark Database used in this paper and the web application providing online access to it were constructed as part of the activities of the German Astrophysical Virtual Observatory as result of a collaboration between the Leibniz-Institute for Astrophysics Potsdam (AIP) and the Spanish MultiDark Consolider Project CSD2009-00064. The BigMD simulation suite have been performed in the Supermuc supercomputer at LRZ using time granted by PRACE. GY and FP acknowledge support from the Spanish MINECO under research grants AYA2012-31101, FPA2012-34694, AYA2010-21231, Consolider Ingenio SyeC CSD2007-0050 and from Comunidad de Madrid under ASTROMADRID project (S2009/ESP-1496).

## REFERENCES

Alimi J.-M., Bouillot V., Rasera Y., Reverdy V., Corasaniti P.-S., Balmes I., Requena S., Delaruelle X., Richet J.-N., 2012, arXiv:1206.2838  
 Angulo R. E., Springel V., White S. D. M., Jenkins A., Baugh C. M., Frenk C. S., 2012, MNRAS, 426, 2046

Angulo R. E., White S. D. M., 2010, MNRAS, 405, 143  
 Baldauf T., Seljak U., Desjacques V., McDonald P., 2012, Phys.Rev.D, 86, 083540  
 Baldauf T., Seljak U., Smith R. E., Hamaus N., Desjacques V., 2013, arXiv:1305.2917  
 Bardeen J. M., Bond J. R., Kaiser N., Szalay A. S., 1986, ApJ, 304, 15  
 Beltrán Jiménez J., Durrer R., 2011, Phys.Rev.D, 83, 103509  
 Berlind A. A., Weinberg D. H., 2002, ApJ, 575, 587  
 Bernardeau F., 1994, ApJ, 427, 51  
 Bouchet F. R., Colombi S., Hivon E., Juszkiewicz R., 1995, Astr.Astrophys., 296, 575  
 Buchert T., 1994, MNRAS, 267, 811  
 Buchert T., Ehlers J., 1993, MNRAS, 264, 375  
 Casas-Miranda R., Mo H. J., Sheth R. K., Boerner G., 2002, MNRAS, 333, 730  
 Catelan P., 1995, MNRAS, 276, 115  
 Cen R., Ostriker J. P., 1993, ApJ, 417, 415  
 Chan K. C., Scoccimarro R., Sheth R. K., 2012, Phys.Rev.D, 85, 083509  
 Coles P., Jones B., 1991, MNRAS, 248, 1  
 de la Torre S., Peacock J. A., 2013, MNRAS, 435, 743  
 Dekel A., Lahav O., 1999, ApJ, 520, 24  
 Desjacques V., Crocce M., Scoccimarro R., Sheth R. K., 2010, Phys.Rev.D, 82, 103529  
 Elia A., Ludlow A. D., Porciani C., 2012, MNRAS, 421, 3472  
 Fry J. N., Gaztanaga E., 1993, ApJ, 413, 447  
 Heß S., et al in prep  
 Heß S., Kitaura F.-S. in prep  
 Heß S., Kitaura F.-S., Gottlöber S., 2013, MNRAS, arXiv:1304.6565  
 Kaiser N., 1987, MNRAS, 227, 1  
 Kim J., Park C., Gott III J. R., Dubinski J., 2009, ApJ, 701, 1547  
 Kitaura F.-S., Jasche J., Metcalf R. B., 2010, MNRAS, 403, 589  
 Kitaura F.-S., 2007, PhD thesis, Ludwig-Maximilians Universität München  
 Kitaura F.-S., Angulo R. E., 2012, MNRAS, 425, 2443  
 Kitaura F. S., Enßlin T. A., 2008, MNRAS, 389, 497  
 Kitaura F.-S., Heß S., 2013, MNRAS, 435, L78  
 Klypin A., Holtzman J., 1997, arXiv:astro-ph/9712217  
 Manera M., Scoccimarro R., Percival W. J., Samushia L., McBride C. K., Ross A. J., Sheth R. K., White M., et al. 2013, MNRAS, 428, 1036  
 Mo H. J., White S. D. M., 1996, MNRAS, 282, 347  
 Mohayaee R., Mathis H., Colombi S., Silk J., 2006, MNRAS, 365, 939  
 Monaco P., Sefusatti E., Borgani S., Crocce M., Fosalba P., Sheth R. K., Theuns T., 2013, MNRAS, arXiv:1305.1505  
 Monaco P., Theuns T., Taffoni G., Governato F., Quinn T., Stadel J., 2002, ApJ, 564, 8  
 Neyrinck M. C., 2013, MNRAS, 428, 141  
 Nuza S. E., Sánchez A. G., Prada F., Klypin A., Schlegel D. J., Gottlöber S., Montero-Dorta A. D., et al 2013, MNRAS, 432, 743  
 Peacock J. A., Heavens A. F., 1985, MNRAS, 217, 805  
 Prada F., et al in prep  
 Prada F., Klypin A. A., Cuesta A. J., Betancort-Rijo J. E., Primack J., 2012, MNRAS, 423, 3018  
 Press W. H., Schechter P., 1974, ApJ, 187, 425  
 Saslaw W. C., Hamilton A. J. S., 1984, ApJ, 276, 13  
 Schneider M. D., Cole S., Frenk C. S., Szapudi I., 2011, ApJ, 737, 11  
 Scoccimarro R., Sheth R. K., 2002, MNRAS, 329, 629  
 Seljak U., 2000, MNRAS, 318, 203  
 Sheth R. K., 1995, MNRAS, 274, 213  
 Sheth R. K., Lemson G., 1999, MNRAS, 304, 767  
 Smith R. E., Scoccimarro R., Sheth R. K., 2007, Phys.Rev.D, 75, 063512  
 Somerville R. S., Lemson G., Sigad Y., Dekel A., Kauffmann G., White S. D. M., 2001, MNRAS, 320, 289  
 Springel V., 2005, MNRAS, 364, 1105  
 Tassev S., Zaldarriaga M., 2012, JCAP, 4, 13  
 Tassev S., Zaldarriaga M., Eisenstein D. J., 2013, J.Cosm.Astr.Phys., 6, 36  
 Valageas P., Nishimichi T., 2011, Astr.Astrophys., 527, A87  
 Watson W. A., Iliev I. T., Diego J. M., Gottlöber S., Knebe A., Martínez-González E., Yepes G., 2013, arXiv:1305.1976